Near-Complete Destruction of PFAS in Aqueous Film-Forming Foam (AFFF) by Integrated Photo-Electrochemical Processes

Yunqiao Guan,[1] Zekun Liu,[2] Nanyang Yang,[1] Shasha Yang,[1] Luz Estefanny Quispe-Cardenas,[1] Jinyong Liu,[2,*] and Yang Yang[1,*]

[1]Department of Civil and Environmental Engineering, Clarkson University, Potsdam, New York 13699, United States

[2]Department of Chemical & Environmental Engineering, University of California, Riverside, California, 92521, United States

*Corresponding author: Email: yanyang@clarkson.edu; Tel: +1-315-268-3861
*Co-corresponding author: Email: jinyongl@ucr.edu; Tel: +1-951-827-1481

ABSTRACT

Per- and polyfluoroalkyl substances (PFAS) are highly recalcitrant pollutants in the water environment worldwide. Aqueous film-foaming foam (AFFF) for fire-fighting is a major source of PFAS pollution. However, complete defluorination (i.e., cleaving all C−F bonds into F^- ions) of PFAS by a non-thermal technology is rare. The destruction of the PFAS mixture in the complex organic matrix of AFFF is even more challenging. In this study, we designed and demonstrated a UV/sulfite−electrochemical oxidation (UV/S−EO) process. The tandem UV/S−EO leverages the complementary advantages of UV/S and EO modules in (i) PFAS transformation mechanism and (ii) engineering process design (e.g., foaming control, chemical dosage, and energy consumption). At ambient temperature and pressure, The UV/S−EO realized near-complete defluorination and mineralization of most PFAS and organics in AFFF (50−500x diluted, containing up to 200 mg L^{-1} organic fluorine and >4000 mg L^{-1} organic carbon). This work highlights the integration of molecular-level insight and engineering design toward solving major challenges of AFFF water pollution and stockpile disposal.

Aqueous film-foaming foam (AFFF) for the suppression of fuel fire is a major cause of the widespread and heavy water environment pollution by per-and polyfluoroalkyl substances (PFAS).[1-6] While substantial efforts have been taken for groundwater remediation, a proactive solution is to contain further PFAS pollution via safe disposal of AFFF stockpiles and decontamination of wastewater from fire-fighting system cleaning.[7, 8] The ideal treatment goal is the complete defluorination of all PFAS in AFFF. However, only hydrothermal approaches have achieved near-complete defluorination of AFFF under supercritical (e.g., 590 °C, 237 atm, 0.1 M KOH, 1 min for 1:100 diluted AFFF)[9] and subcritical conditions (e.g., 350 °C, 163 atm, 5 M NaOH, 30 min for 1:2 diluted AFFF).[10, 11] Therefore, a non-thermal and cost-effective technology for complete PFAS defluorination is still highly desirable.

Although the information on AFFF ingredients remains largely proprietary, the PFAS-based surfactants are generally composed of a fluoroalkyl moiety (R_F) and an organic moiety (R_O).[12-14] The two moieties are connected by either sulfonamide ($R_F{-}SO_2NH{-}R_O$) or hydrocarbon telomer linkers ($R_F{-}(CH_2)_m{-}R_O$). From the perspective of chemical degradation, most such surfactants can be hydrolyzed or partially oxidized into perfluoroalkane sulfonates (PFSAs, $C_nF_{2n+1}{-}SO_3^-$), perfluorocarboxylates (PFCAs, $C_nF_{2n+1}{-}COO^-$), and fluorotelomer acids (FTs, $C_nF_{2n+1}{-}(CH_2)_m{-}X$). However, most non-thermal technologies reported to date cannot achieve complete defluorination of all PFAS structures. The degradability of individual PFAS depends on the specific molecular structure, particularly the end functional group and fluoroalkyl chain length.[15, 16] For example, the homogeneous ultra-violet/sulfite (UV/S) treatment shows low efficiency in destroying short-chain FTs and PFSAs due to their low intrinsic reactivity with hydrated electrons (e_{aq}^-).[17, 18] The heterogeneous plasma treatment is not good at destroying short-chain PFAS because they do not accumulate at the reactive gas-liquid interface.[16, 19] Previously reported heterogeneous electrochemical oxidation (EO) treatment also exhibited various mass transfer and reactivity limitations in destroying individual PFAS structures.[20-22] The rich contents of organic solvents and hydrocarbon surfactants in AFFF further challenge the efficacy and efficiency of the PFAS destruction systems.[23]

Building upon the insights into both UV/S and EO technologies, we developed a UV/S−EO tandem process to maximize the strength and overcome the limitation of each module. At ambient temperature and pressure, the UV/S−EO treatment achieved ~100% defluorination efficiency (DeF) of various individual PFAS chemicals and the mixed PFAS in diluted AFFF (1:50−1:500, corresponding to 20−200 mg L^{-1} of total fluorine). In this report, we present the process design rationales, demonstrate the system performance, and elucidate the reaction mechanisms. The findings provide a widely applicable solution for mineralizing mixed PFAS in various water treatment scenarios.

Process Design Rationales.

Our previous studies have revealed that UV/S is highly effective in destroying long-chain PFCAs and PFSAs (n>4 for the $C_nF_{2n+1}{-}$ moiety) but sluggish for short-chain (n≤4) PFSAs and FTs.[17] Moreover, UV/S treatment alone cannot achieve complete defluorination for most structures. One of the major pathways, reductive hydrodefluorination (i.e., $C{-}F + 2\ e_{aq}^- + H^+ \rightarrow C{-}H + F^-$), can generate segregated fluorocarbons moieties (e.g., $CF_3{-}CH_2{-}X$). The high C−F bond dissociation energy and the lack of favorable neighboring groups (e.g., $-COO^-$) prevent further defluorination. In a proof-of-concept study, post-oxidation of the UV/S treated residues achieved near-complete overall defluorination for most PFAS.[18, 24] For practical engineering, the

oxidative power must be delivered by a cost-effective technology (e.g., EO) rather than heat-activated persulfate oxidation. EO with the boron-doped diamond (BDD) electrode has demonstrated effective destruction of a wide range of PFCAs, PFSAs, and FTs, with a robust performance in various water matrices and a lower sensitivity to PFAS structures than UV/S.[20, 25, 26] However, direct application of EO on individual PFAS or diluted AFFF did not achieve complete defluorination (see the next section). It appears that UV/S and EO mechanistically complement each other toward complete defluorination.

To probe the suitability of integrating UV/S and EO, we conducted a density functional theory (DFT) based calculation to compare the oxidizability of PFOA anion ($C_7F_{15}-COO^-$) and its representative hydrodefluorinated product after UV/S treatment, $C_7F_{14}H-COO^-$. The calculation adopted the Marcus theory to estimate the activation enthalpy of these two structures to lose one electron, which simulates the PFAS destruction via direct electron transfer to the anode.[27, 28] The results indicate that $C_7F_{14}H-COO^-$ is more vulnerable to EO than PFOA as the activation enthalpy profile moves toward lower anodic potentials (Text S1 and Fig.S1). In contrast, the $C_7F_{14}H-COO^-$ degradation under UV/S treatment was much slower than PFOA.[17, 18] Therefore, the tandem UV/S−EO treatment train is mechanistically favorable.

Besides the molecular-level insights, a series of process engineering considerations also consolidate the system design that places UV/S before EO. If EO is placed before UV/S, the direct treatment of perfluorinated structures can generate short-chain PFCA products that UV/S cannot achieve 100% defluorination. Second, EO treatment often generates dissolved oxygen, oxyanions, and even free chlorine, consuming sulfite in the following UV/S. Third, EO treatment of diluted AFFF generates high and dense foams that can incur various operational challenges (Fig.S2). But the UV/S−EO layout effectively addresses the foaming issues (to be highlighted in the following content). Fourth, Na_2SO_3 added in UV/S can be an electrolyte and source of sulfate radicals in the downstream EO treatment, thus minimizing chemical consumption.

Novel Structure-Defluorination Relationships in EO Treatment.

We used BDD, the gold-standard EO electrode material, to treat the diverse PFAS and organics in AFFF. This study used a plate-type microcrystalline BDD electrode (16 cm^2; Fig. S3a) with dopant densities of 3×10^{20} boron atoms cm^{-3}.[29] The potential concerns about byproduct formation are addressed in the last section. The first step was to systematically probe the structure-defluorination relationship for AFFF-relevant PFAS, including n=1−8 $C_nF_{2n+1}-COO^-$ (PFCA), n=4,6,8 $C_nF_{2n+1}-SO_3^-$ (PFSA), and n=4,6,8 $C_nF_{2n+1}-CH_2CH_2-SO_3^-$ (FTS). The BDD EO treatment showed excellent performance for all structures. Except for $C_4F_9-SO_3^-$ (perfluorobutane sulfonate, PFBS), most PFAS showed complete parent structure degradation within 2 h (Fig.1a,b). Because no aqueous radicals (e.g., HO• and SO_4^-•) can react with $C_nF_{2n+1}-SO_3^-$, the degradation must have been initiated by the direct electron transfer from PFAS molecule to BDD electrode surface (i.e., a heterogeneous process). Thus, the slower degradation of the shorter PFSA (Fig.1b) can be attributed to the higher solubility in water. However, the same trend of mass transfer limitation was not observed on short-chain n=1−4 $C_nF_{2n+1}-COO^-$ because EO can generate aqueous SO_4^-• from sulfate-containing electrolytes.[30, 31] SO_4^-• can also initiate PFCA degradation by decarboxylation.[24, 30]

The EO treatment achieved deep defluorination (i.e., 60−100%) for all PFAS structures. We also observed several interesting trends. For PFCAs, n=1,2,4,6 allowed significantly higher defluorination than n=3,5,7,8 (Fig.1c). For PFSAs and FTSs, n=4 and 6 of both categories allowed

near complete defluorination, whereas the two n=8 structures are defluorinated by 65% (Fig.1d). These disparities suggest that the reaction mechanisms go beyond the previously known "zipping-off" mechanism, where the removal of terminal functional groups (i.e., $-COO^-$, $-SO_3^-$, and $-CH_2CH_2-SO_3^-$) exposes the $R_F-CF_2\bullet$ for stepwise defluorination of the two C–F bonds and oxidation of the carbon into CO_2 (Fig.1e).[32, 33] The odd/even number of $-CF_2-$ in PFCAs appears to have interesting effects on the gap from 100% defluorination (<10% for *n*=2,4,6 versus >20% for *n*=3,5,7 $C_nF_{2n+1}-COO^-$). It is also very interesting to observe the much lower defluorination from all three *n*=8 structures than their *n*=2 and 4 analogs. Elucidating the underlying mechanisms go beyond the scope of this work but definitely warrants further study.

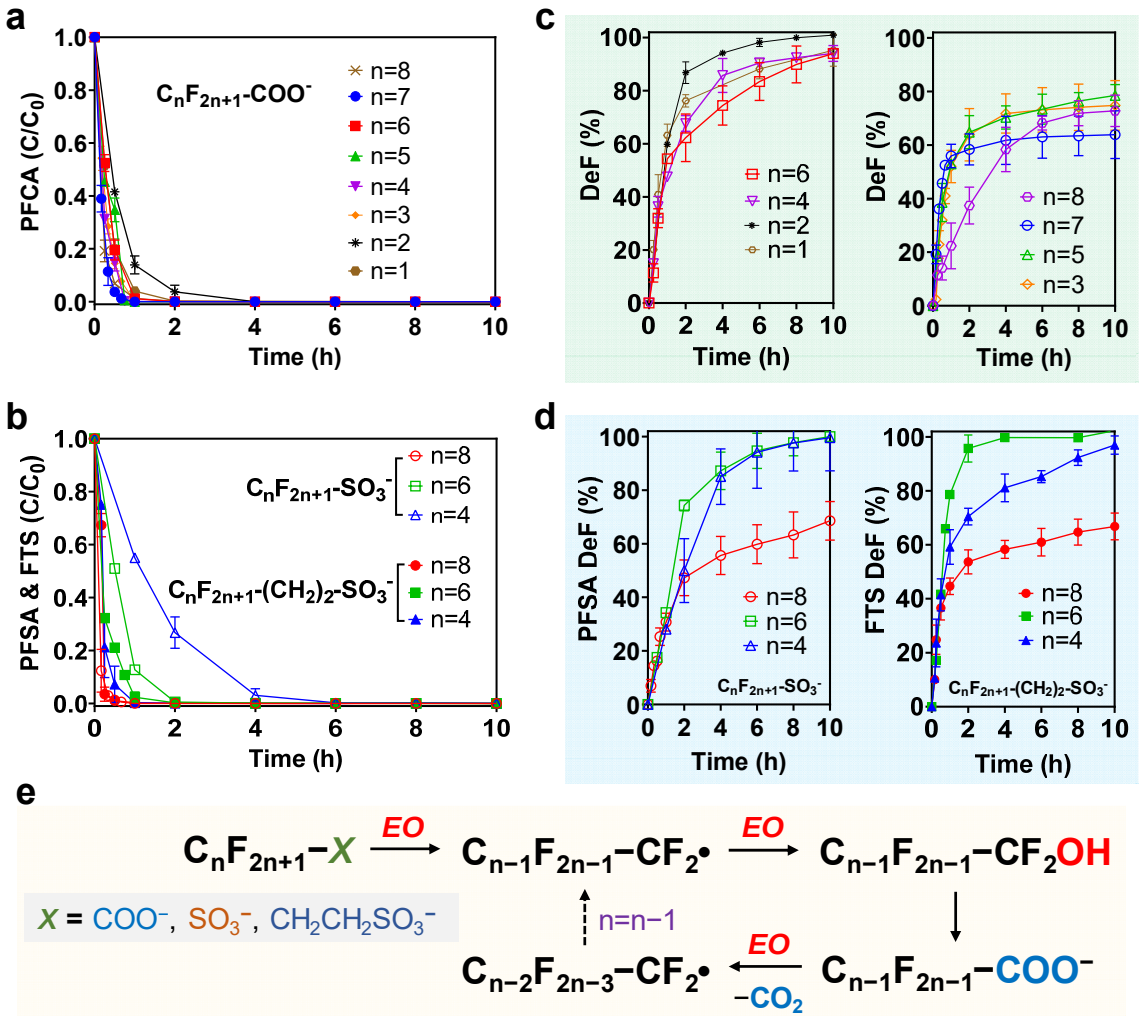

Fig. 1. Parent compound degradation and defluorination of **(a+c)** n=1–8 PFCA, **(b+d)** n=4,6,8 PFSA and FTS by EO treatment and the previously known "zipping-off" pathway. Reaction conditions: individual PFAS (25 µM, except 1000 µM for TFA for the ease of F^- measurement) spiked in 20 mL water with 100 mM Na_2SO_4 as electrolyte; current density of 15 mA/cm^2 applied to a 16 cm^2 BDD anode. Data are presented as mean values of triplicates ± standard deviation.

For the degradation of individual PFAS structures, EO has an overwhelming advantage over UV/S. The strongly oxidative environment rapidly destroyed *n*=4 FTS and achieved >95% defluorination. But this compound is highly recalcitrant under UV/S[18, 24] because the short C_4F_9-

moiety segregated by the $-CH_2CH_2-$ linker does not have a weak C−F bond for easy defluorination by e_{aq}^-.[17] This experimental finding corroborates the insights from the DFT calculation discussed in the earlier section. Moreover, in comparison to UV/S, EO achieved much faster (10 h versus >24 h) and deeper (~100% versus 78%) defluorination of PFBS.[18, 24] Hence, EO has higher tolerance with short-chain PFAS than two other heterogeneous technologies- plasma and sonication- both encountered challenges from PFBS ($C_4F_9-SO_3^-$) and PFBA ($C_3F_7-COO^-$).[34, 35]

Based on the above experimental findings, we hypothesized that EO could be placed after UV/S to obtain the best treatment result for multiple reasons. First, EO can achieve ~100% defluorination of $n \leq 4$ short-chain FTs and PFSAs, which are much more sluggish under UV/S treatment. Second, although EO cannot achieve 100% defluorination from n=3,5,7,8 PFCA, UV/S can rapidly defluorinate these structures by 82−93%. The remnant C−F bonds are in the recalcitrant H-rich residues after UV/S. But these residues are ideal substrates for EO destruction. Third, although EO cannot achieve 100% defluorination from n=8 PFSA and FTS, UV/S provides efficient conversion of weak C−F bonds in the long $C_8F_{17}-$ moiety to C−H, or cleave the middle C−C bonds to yield shorter-chain FT products,[17] which appear to be ideal substrates for 100% defluorination by EO.

UV/S−EO treatment of Individual PFAS Compounds.

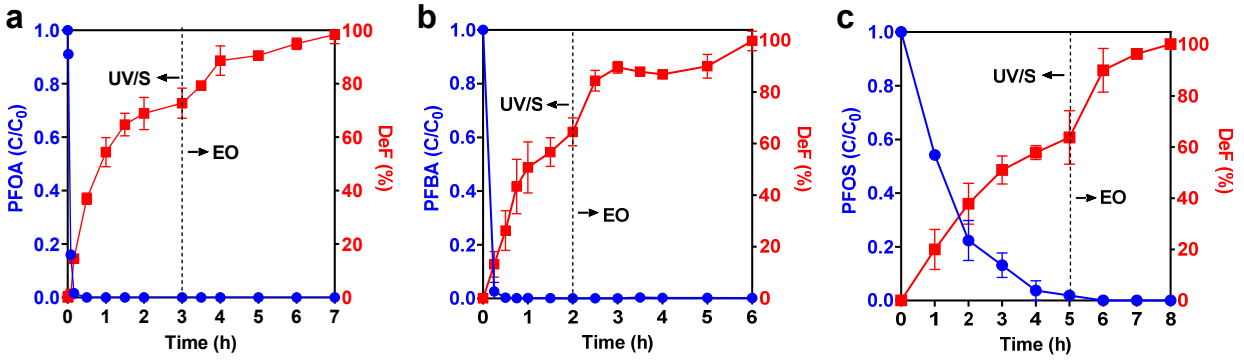

Fig. 2. UV/S−EO degradation and defluorination of **(a)** PFOA, **(b)** PFBA, and **(c)** PFOS. Reaction conditions for UV/S: individual PFAS (25 μM) spiked in 750 mL of water, 10 mM Na_2SO_3, and a 16 W low-pressure Hg lamp. The following EO treatment used the same conditions described in the caption of **Fig. 1**. Data are presented as mean values of triplicates ± standard deviation.

To validate the hypotheses above, we developed a primitive UV/S−EO layout to treat PFOS, PFOA, and PFBA, all of which are representative PFAS and could not be 100% defluorinated by EO (Fig.1). In the first stage of UV/S treatment, PFOA and PFBA were completely removed within 30 min (Fig.2a,b). After the parent PFCAs quickly disappeared, the defluorination from the transformation products continued. In previous studies, the maximum defluorination from PFCAs under the same UV/S condition took 4−8 h.[36] However, for the UV/S−EO layout, we arbitrarily stopped the UV/S treatment after 2−3 h when the increase of defluorination became sluggish. For the more recalcitrant PFOS under UV/S treatment, the defluorination accompanied the parent compound removal.[24] We stopped UV/S when most parent PFOS disappeared at 5 h (Fig.2c). The following EO treatment increased defluorination to 100% for all three PFAS.

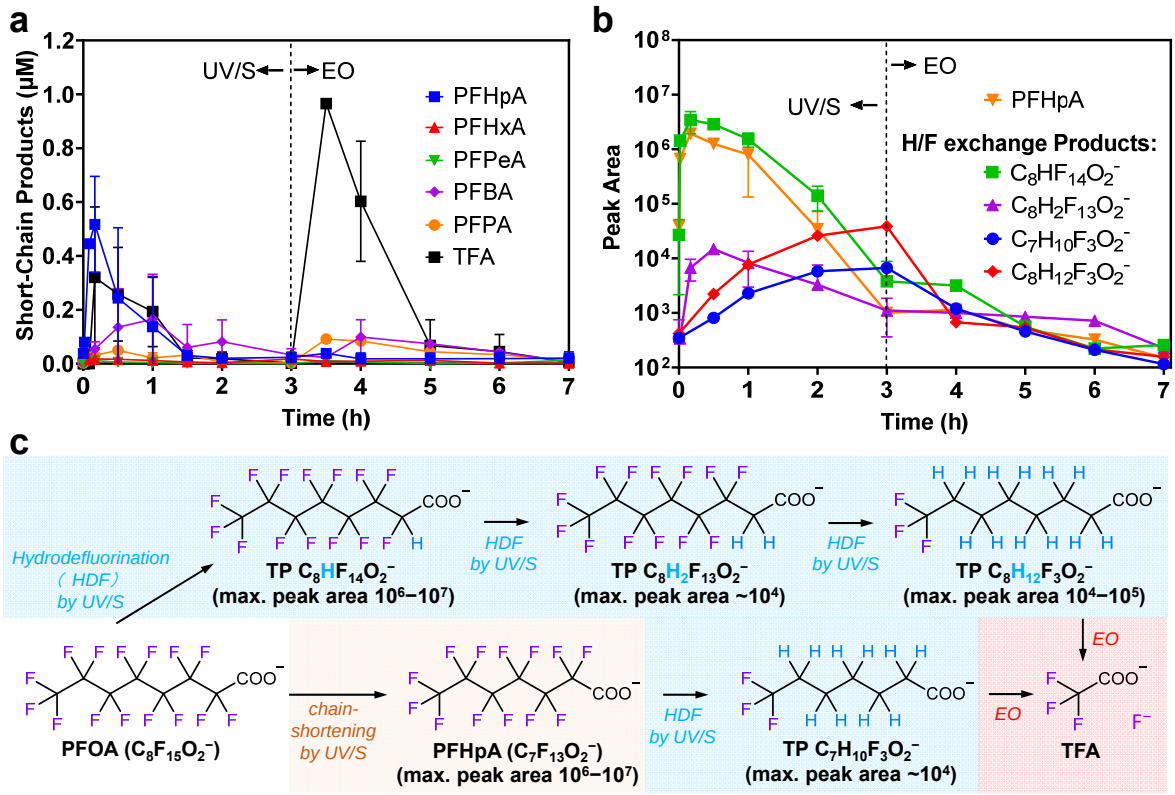

Fig. 3. Evolution of detected transformation products during the UV/S−EO treatment of 25 μM PFOA: **(a)** short-chain (SC) PFCAs and **(b)** non-target analysis of hydrodefluorinated products. Data are presented as mean values of triplicates ± standard deviation. **(c)** Formation pathways for representative products.

Transfomration product (TP) analyses verified our mechanistic hypotheses. The UV/S treatment of *n*=7 PFOA generated a series of shorter-chain *n*=1−6 PFCAs (Fig.3a) as quantified by a triple-quadrupole mass spectrometer (QQQ MS/MS). These PFCAs are attributed to the well-known decarboxylation[17] and a recently identified C−C bond cleavage mechanism.[37] The UV/S treatment removed most of the PFCA TPs within 3 h. Quadruple time-of-flight high-resolution mass spectrometer (Q-ToF-HRMS) found a series of hydrodelfuorination products (Fig.3b) from the parent PFOA ($C_8F_{15}O_2^-$) and the chain-shortened PFHpA ($C_7F_{13}O_2^-$). The MS peaks for $C_8HF_{14}O_2^-$ and PFHpA showed similar abundance, indicating that the two transformation pathways proceeded in parallel and were equally significant (Fig.3c). The UV/S degradation of hydrofluorinated TPs, such as $C_8HF_{14}O_2^-$ and $C_8H_2F_{13}O_2^-$, were much slower than the perfluorinated PFOA (Fig.3b versus Fig.2a). The detection of deeply hydrodefluorinated TPs (e.g., $C_8H_{12}F_3O_2^-$ and $C_7H_{10}F_3O_2^-$) is consistent with the previous study using a different photoreactor setting and a quadrupole Orbitrap HRMS instrument.[38] The three residual C−F bonds with high recalcitrance against UV/S were most probably on the terminal CF_3−. The switch to EO mode generated short-chain PFCAs again (Fig.3a) from various hydrodefluorinated TPs. The sharp increase of TFA suggested that hydrodefluorination by UV/S occurred on carbon atoms near the terminal CF_3−. With the extension of EO treatment, all PFCA TPs (Fig.3a) and hydrodefluorinated TPs (Fig.3b) were destroyed to negligible concentrations, as evidenced by the defluorination to ~100% (Fig.2a).

UV/S−EO treatment of AFFF.

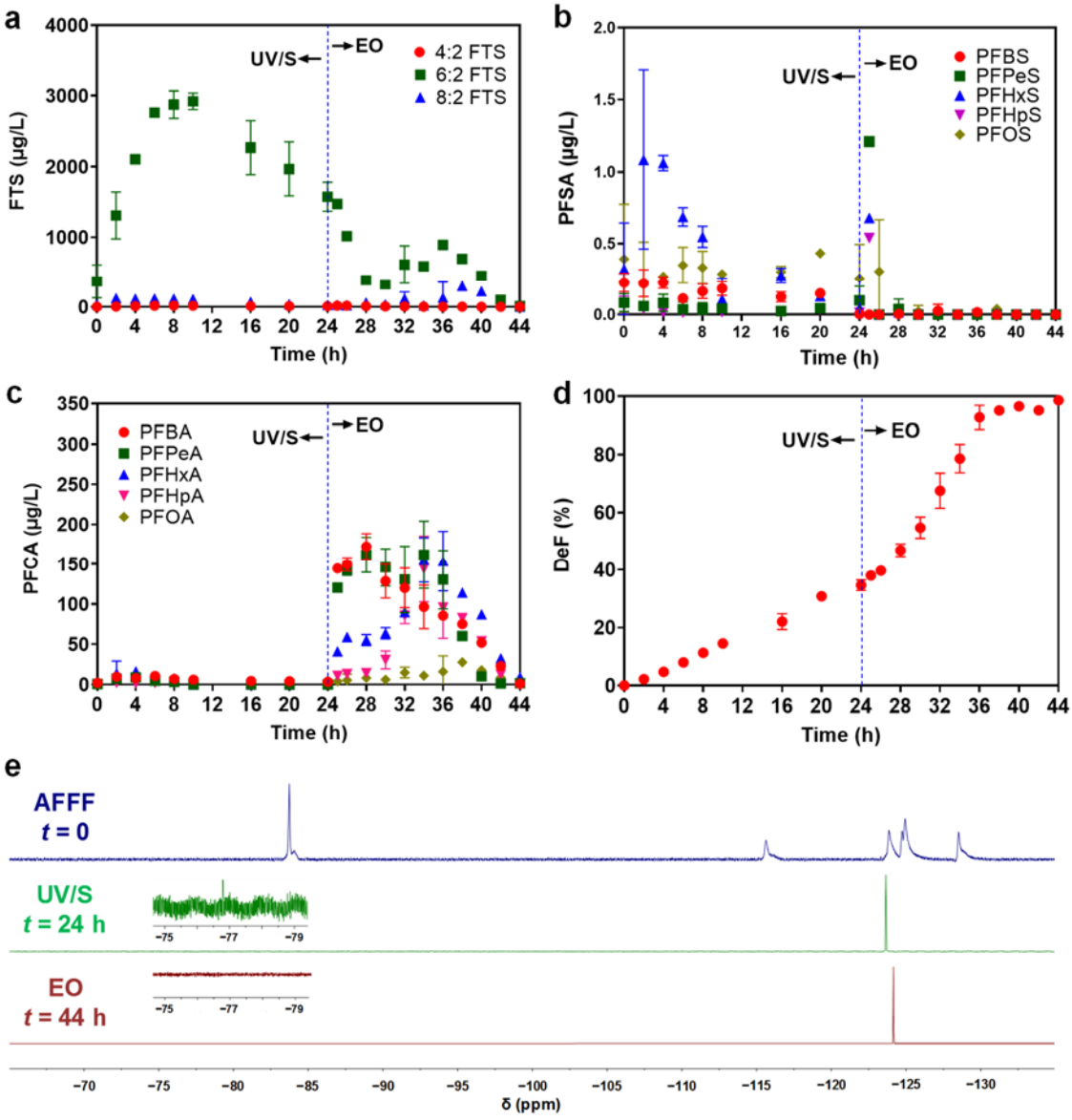

Fig. 4. Time profiles of **(a)** FTS, **(b)** PFSA, **(c)** PFCA, and **(d)** defluorination during UV/S−EO treatment of AFFF (1:100 diluted in DI water; $[TOF]_0$ = 103 mg L^{-1}). Reaction conditions for UV/S: 750 mL of water, 100 mM Na_2SO_3, pH 12 by NaOH, and a 16 W low-pressure Hg lamp. The EO treatment (no Na_2SO_4 added) was conducted in a BDD flow cell at a current of 5 A and an average cell voltage of 25 V. Data are presented as mean values of triplicates ± standard deviation.

The near-quantitative defluorination of individual PFAS structures motivated us to apply UV/S−EO for AFFF treatment at ambient conditions. For fire suppression, the original AFFF liquid was typically diluted about 100-fold. It was further diluted after entering the water environment. To date, only a few studies have reported treating diluted AFFF (total fluorine 0.16−27 mg L^{-1}) by individual EO, UV/S, and plasma technologies.[21, 39, 40] None of these non-thermal methods realized ~100% defluorination (Table S3).[41]

The total fluorine in the original AFFF was measured as 10 g L^{-1} by combustion ion chromatography (Table S1). Nineteen of the 30 targeted PFAS structures were detected in AFFF by QQQ MS/MS (Table S2). The three most abundant targeted PFAS were 6:2 FTS (139 mg L^{-1}), 8:2 FTS (7.85 mg L^{-1}), and PFOA (3.54 mg L^{-1}). However, F elements from all targeted PFAS only accounted for 2% of the total fluorine. ^{19}F nuclear magnetic resonance (NMR) analysis found the dominant species in AFFF as *n*=6 FT surfactants (i.e., $C_6F_{13}-(CH_2)_m-R_O$, Fig. S4), but the structure of the organic moiety (R_O) was unknown. We hypothesized that the surfactants could be defluorinated via similar mechanisms as for individual PFAS with the same R_F building blocks (Fig.1d). Hence, to effectively monitor the treatment process, we kept tracking the concentrations of FTSs, PFSAs, PFCAs, select surfactant molecules,[10, 14] and F^- ion (Fig.4).

Under UV/S treatment of the 100-fold diluted AFFF (total fluorine at 100 mg L^{-1}), the concentration of 6:2 FTS increased in the first 8 hours and then slowly decreased (Fig.4a). PFSAs such as the C6 PFHxS, although in low concentrations, showed a similar generation-degradation profile (Fig.4b). It exhibited higher recalcitrance than that observed in previous studies using pure PFHxS in the deionized water matrix.[24] The slow apparent degradation of these species can be attributed to (1) competing species in the organic matrix of diluted AFFF[23] and (2) the continuous generation of PFHxS from *n*=6 sulfonamide surfactant precursors. This reasoning is further supported by the rather consistent concentration of PFOS, which has higher reactivity than PFHxS in previous UV/S studies.[24] The sustained PFOS throughout the 24 h is most probably attributed to the conversion of *n*=8 sulfonamide precursors. PFCAs also showed generation-degradation patterns under UV/S treatment (Fig.4c). Because the initial concentrations of all PFCAs were negligible, the generated PFCAs could be attributed to the conversion of fluorotelomeric and sulfonamide precursors.[17] A series of *n*=4−7 surfactant molecules (detected by Q-ToF-HRMS following literature[10]) demonstrated high recalcitrance or even net increase (Fig.S5). The UV/S module resulted in 40% of overall defluorination after 24 h (Fig.4d). Extended reaction beyond 24 h did not further increase defluorination (Fig.S6).

After switching to EO mode, all surfactant molecules degraded to non-detected after 40 h (i.e., 16 h under EO, Fig.S5). In comparison, most targeted PFAS structures showed concentration increases sooner or later (Figs.4a,b,c), and eventually became non-detected after 44 h (i.e., 20 h under EO). In particular, elevated PFCAs showed the generation-degradation profiles in a wide time window (Fig.4c versus Fig.1a), indicating the oxidative transformation of the abundant FT surfactants. The early generation of *n*=5 PFHxA, *n*=4 PFPeA, and *n*=3 PFBA in high concentrations suggest the oxidative conversion of the dominant *n*=6 FT precursors, as revealed by ^{19}F NMR (Fig. S4). The oxidation of pure *n*=6 FTS using HO• radicals yielded similar PFCA product distributions (i.e., "*n*−2 dominance" rule).[24, 42] The second wave of PFCA generation started after 32 h, with the most significant increase for *n*=6 PFHpA, followed by *n*=5 PFHxA and *n*=7 PFOA, suggesting a slower oxidative conversion of *n*=8 FT precursors.[24, 42] The increase of *n*=6 and 8 FTSs during EO treatment (Fig.4a) suggested the oxidation of organic moieties. The very short time window for PFSAs (Fig.4b) further confirmed that sulfonamide precursors were minor components in the studied AFFF, and all degraded within a few hours. After the EO treatment, all targeted PFAS were below the detection limits shown in Table S2. The F^- ion release reached ~100% of overall defluorination (Fig.4d). ^{19}F NMR analysis of the residual also found no other F resonance beside F^- (Fig.4e), which is another evidence for the near-quantitative defluorination.

Engineering considerations for AFFF treatment by UV/S−EO.

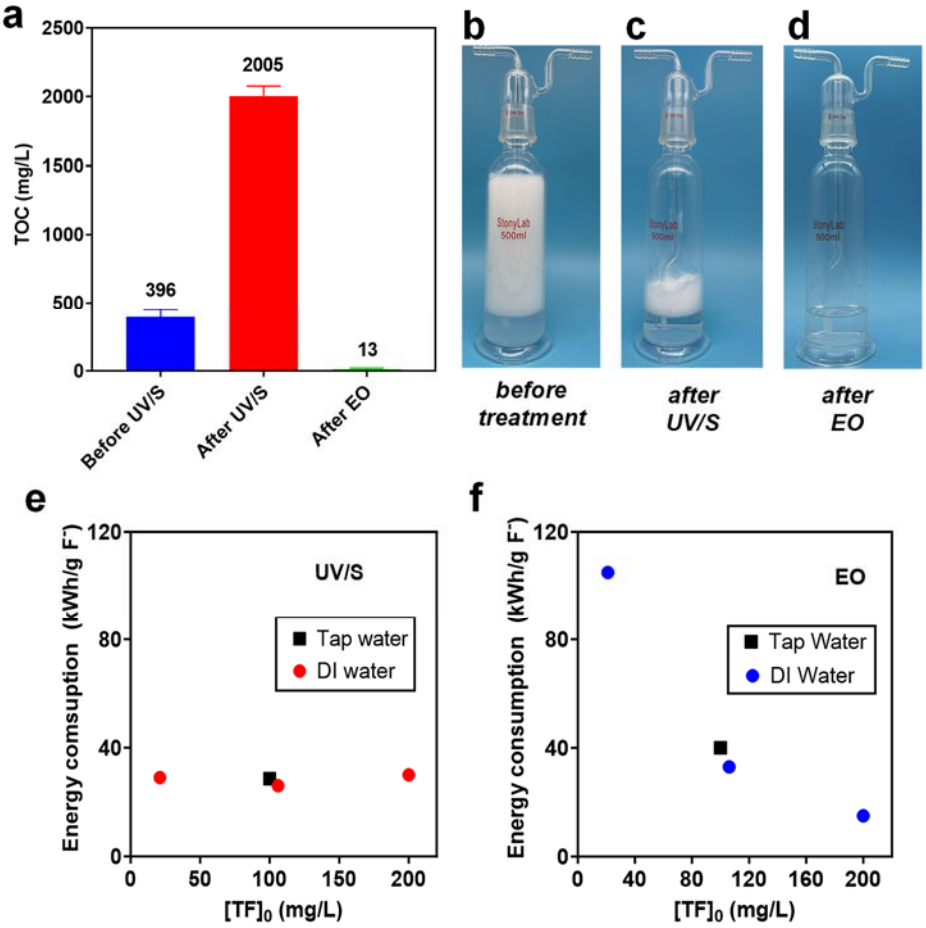

Fig. 5. (a) Measured TOC and **(b−d)** foaming potentials of the 1:100 diluted AFFF in DI water before and after different treatment steps. The 500 mL gas washing bottle was loaded with 70 mL of each water sample. Air was purged through the glass frit immersed in the aqueous phase (2.5 cm deep) till a stable foam layer was observed. The heights of the foam layer for the three samples were 15, 3.6, and 0 cm, respectively. Energy consumption of **(e)** UV/S and **(f)** the following EO at different $[TF]_0$.

TOC removal. Besides the 10 g L^{-1} of organic fluorine, AFFF contained heavy amounts of hydrocarbon surfactants.[43] Total organic carbon (TOC) analysis of the 100-fold diluted AFFF found 396 mg L^{-1} of organic carbon (Fig.5a). However, after UV/S treatment, the measured TOC increased to 2005 mg L^{-1}. Notably, the combustion temperature of the TOC analyzer by default setting (680 °C) cannot thoroughly oxidize all carbons, especially the fluorinated carbons, into CO_2. Hence, UV/S treatment converted the "combustion-proof" mixed surfactants into more thermally oxidizable structures. After EO treatment, TOC was drastically reduced to only 13 mg L^{-1}. Assuming the value of 2005 mg L^{-1} was similar to or still lower than the actual TOC of the 100-fold diluted AFFF, the TOC removal by EO was ≥99.4%. Because fluorinated carbon that accommodates 100 mg L^{-1} of organic F as CF_2 and CF_3 was only a small portion of TOC, we concluded that EO treatment allows very deep mineralization of most hydrocarbon surfactants. Therefore, if organic removal is needed for AFFF treatment at ambient conditions, EO is a highly competitive technology option.

Foam suppression. Although EO provides a strong capability of mineralizing both organic and fluorinated carbons in AFFF, direct EO treatment encountered a serious foaming issue due to the vigorous gas evolution from water-splitting reactions (Fig.S2). To quantitatively describe the foaming, we arbitrarily define the "foaming potential" as the ratio between the height of foam and the depth of liquid under air purging at 100 mL min^{-1}. Before treatment, the 100-fold diluted AFFF had a foaming potential of 6 (Fig.5b). After UV/S treatment, the value decreased to 1.4 (Fig.5c), allowing an easy operation of EO treatment. We only observed a thin foam layer with a height of less than 8% of the liquid in the first 4 h and no foaming thereafter. As expected from the ≥99.4% TOC removal, the foaming potential became zero after the EO treatment (Fig.5d). Therefore, the sequential UV/S−EO has a unique advantage in addressing the foaming issue from AFFF treatment.

Robustness in real-world scenarios. An imminent application scenario is the cleaning of hanger fire-fighting pipelines and fire trucks that used PFAS-based AFFF in the past decades.[7, 8] This time, we used tap water for the 100-fold dilution of AFFF (Table S1). The UV/S−EO treatment resulted in very similar evolution/degradation kinetics for all individual PFAS and F^- release (Fig.S7) to the DI water diluted AFFF (Fig.4). We also observed very similar reaction kinetics for all species at the dilution factors of 50 (Fig.S8) and 500 (Fig.S9), except that the more diluted (i.e., less concentrated) AFFF needed less time to achieve 100% defluorination. For the UV/S module, the chemical and energy consumption appeared proportional to the dilution factor (Fig.S8d versus S9d). The treatment of 500-fold diluted AFFF needed 10 mM sulfite and 12 h to reach the maximum defluorination of 46%. For the 50-fold diluted AFFF, 100 mM sulfite and 120 h were needed to reach the maximum defluorination of 48%. In comparison, the EO module is less sensitive to the dilution factor. The time required to achieve the 100% overall defluorination for 50- and 500-fold diluted AFFF was 24 and 12 h, respectively. It is important to highlight that the 50-fold diluted AFFF had a record-high TOC > 4000 mg L^{-1} and TOF at 200 mg L^{-1} compared with those samples treated in the previous studies (Table S3). Hence, the UV/S−EO has demonstrated great promise to destroy concentrated PFAS in wastewater, particularly for the major challenges in fire-fighting system cleaning and AFFF disposal (after adequate dilution).

Energy consumptions. We calculated the energy efficiency of UV/S and EO modules based on the slopes of the quasi-linear segments of the defluorination profiles (Figs.4d, S7d, S8d, and S9d) as the required energy input (kWh) to convert per gram of the organic fluorine to F^- (Figs. 5e and 5f). The light-adsorbing water matrices are usually expected to limit the efficacy of photochemical systems,[44] but the UV/S system exhibited a consistent energy efficiency for the 50-, 100-, and 500-fold diluted AFFF. In particular, the UV/S treatment further reduced the absorbance at 254 nm in the 50-fold diluted AFFF from 1.36 to 0.36 (Table S4). This "self-sharpening" feature makes UV/S suitable for treating concentrated AFFF. The lowest dilution factor of 1:50 in this work is three orders of magnitude lower (i.e., three orders of magnitude more concentrated) than the previous UV/S demonstration, which diluted AFFF 60,000-fold and operated at pH 9.5.[23] The limited dilution substantially reduced the water volume to be treated, thus substantially saving the electrical energy for UV irradiation.

For EO treatment, the energy consumption decreased with the lower dilution factor. This observation aligns with the principle of heterogeneous catalysis: the higher bulk concentration creates a steeper concentration gradient at the water/electrode interface, thus enhancing the mass transfer of PFAS to the BDD surface and the subsequent oxidation by direct electron transfer.

Therefore, limited dilution, though deemed challenging in many treatment processes, is highly beneficial for improving the electrical energy efficiency of the EO module.

Extended discussion toward practical applications.

The UV/S−EO tandem process achieved the long-pursued goal of near-quantitative defluorination of PFAS as either individual chemicals or a complex mixture in the AFFF matrices. The process design was built on the state-of-the-art understanding of the complementary capabilities of the two modules: 1) UV/S is highly effective for defluorinating long-chain PFAS that EO could not defluorinate to 100%; 2) EO is highly effective in mineralizing short-chain PFAS and H-rich TPs from UV/S treatment, both of which are recalcitrant under UV/S; and 3) UV/S treatment effectively suppressed foaming that could cause operational issues for EO. Moreover, both UV/S and EO exhibited high energy efficiency in treating AFFF with limited dilution. EO also enabled the near-complete removal of TOC in AFFF. All reactor components are commercially viable at full-scale. The integration only requires conveying the treated effluents without retrofitting the reaction units. We expect this treatment strategy to be also effective toward novel PFAS structures[37, 38, 45] in various practical scenarios under ambient conditions.

Lastly, we emphasize that UV/S−EO was developed for the non-potable treatment of obsolete AFFF stockpiles and fire-fighting system cleaning solutions. Therefore, the concern about the disinfection byproducts, which are only regulated in the drinking water supply, should not constrain the improvement and deployment of the process. Besides, technologies for removing halogenated byproducts and oxyanions are widely available and can be adopted as post-treatment add-ons.[46-48] We are developing various engineering processes with pre- and post-treatment that can further expand the application scope of UV/S−EO in even more challenging water matrices.

Methods

Chemicals. Chemicals used as received include sodium sulfite (Sigma-Aldrich, ≥98%), sodium hydroxide (J.T.Baker, ≥99%), sodium sulfate (J.T.Baker, ≥98%), PFCAs (n = 1−8 $C_nF_{2n+1}COO^-$), PFSAs (n = 4,6,8 $C_nF_{2n+1}SO_3^-$), and FTSAs (n = 4,6,8 $C_nF_{2n+1}-CH_2CH_2-SO_3^-$)were used as received. The information on CAS numbers, purities, and vendors is collected in the Supporting Information (Table S5).

Analysis. Targeted analysis of PFAS was conducted on ultra-high-performance liquid chromatography (UPLC, Thermo Vanquish) coupled to a triple quadrupole mass spectrometer (QQQ MS/MS, Thermo Altis). The analytical method includes 30 PFAS. Details of instrument setup were described in our previous publication.[49] Nontargeted analysis of PFAS transformation products was performed on high-performance liquid chromatography-quadrupole time-of-flight mass spectrometry (HPLC/Q-ToF-MS, SCIEX). The instrument setup was described in Text S2. The search and match of unknown fluorocarbon structures follow the protocol developed previously.[41]

The F^- was quantified by ion chromatography (IC). The TF of AFFF was analyzed by combustion ion chromatography (CIC; Metrohm), with the principle of decomposing AFFF samples at 1050 °C and using an IC to measure the F^- released. Details were described previously.[39, 49]

The defluorination efficiency (DeF) for the treatment of a single PFAS target was calculated as follows:

353 $$DeF = \frac{C_{F^-}}{C_0 \times N_{C-F}} \times 100\%$$

354 where C_{F^-} is the molar concentration of F^- ion released in solution, C_0 is the initial molar
355 concentration of the parent PFAS, and N_{C-F} is the number of C−F bonds in the parent PFAS
356 molecule.

357 The DeF for the treatment of diluted AFFF was obtained via:

358 $$DeF = \frac{C_{F^-}}{C_{TF} - C_{F^-,0}} \times 100\%$$

359 Where C_{TF} and $C_{F^-,0}$ are the concentrations of total fluorine and F^- (if any) in the diluted AFFF.

360 ***UV/S treatment.*** A customized 750 mL stainless steel photoreactor with quartz UV-lamp
361 sheath and a 16 W low-pressure mercury lamp (254 nm narrowband irradiation) were used for
362 UV/S treatment photon flux ($1.3 \pm 0.2\times10^{-6}$ E s^{-1}), effective path length (27 cm), and average
363 (5.4×10^{-8} E·s^{-1}·cm^{-2}) were determined using the established methods (Text S3).[50] For the UV/S
364 treatment of a single PFAS, the DI-water was spiked with 25 μM target PFAS and 10 mM Na_2SO_3.
365 The pH was adjusted to 12 by 1 M NaOH to achieve the highest photo-reductive treatment
366 efficiency.[36] As for the UV/S treatment of AFFF, AFFF samples diluted by DI water or tap water
367 at ratios of 1 to 50, 1 to 100, and 1 to 500 were amended with Na_2SO_3 at 100, 100, and 10 mM,
368 respectively. The reactor was sealed from the air without inert gas protection in all tests.

369 ***EO treatment***. EO treatment based on plate-type BDD (Element Six; Fig S3a) aims to
370 evaluate the treatability of target PFAS with or without UV/S pretreatment. In these tests, 20 mL
371 PFAS-containing electrolytes with or without UV/S pretreatment were electrolyzed in batch mode
372 by a 16 cm^2 BDD anode coupled with a stainless-steel cathode at 15 mA/cm^2, corresponding to a
373 total current of 0.24 A.

374 In order to establish the proof-of-concept UV/S−EO tandem treatment train, we adopted a
375 BDD flow cell for a larger treatment capability. The BDD flow cell reactor provided by Element
376 Six contains two BDD disks (Ø 4.4 cm each at an interspace of 0.8 cm) that serve as anode and
377 cathodes (Fig. S3b). The flow cell has a chamber volume of 95 mL. In the tandem treatment
378 process, 750 mL of diluted AFFF will be first subjected to UV/S reductive treatment; the 750 mL
379 treated water will then be circulated through the flow cell at a flow rate of 100 mL/min. It is
380 important to note that the batch EO tests using plate-type BDD have a current-to-volume ratio of
381 12 A/L. If the same ratio is replicated in the flow cell setup, the required total current is 9 A to
382 treat 750 mL. However, limited by the capacity of the bench-scale power supply, the flow cell was
383 operated at 5 A, corresponding to a current density of 329 mA/cm^2. The near-complete
384 defluorination of AFFF was achieved in the compromised condition, nonetheless.

385

REFERENCES

1. Evich, M. G.; Davis, M. J.; McCord, J. P.; Acrey, B.; Awkerman, J. A.; Knappe, D. R.; Lindstrom, A. B.; Speth, T. F.; Tebes-Stevens, C.; Strynar, M. J., Per-and polyfluoroalkyl substances in the environment. *Science* **2022,** *375*, eabg9065.

2. Moody, C. A.; Field, J. A., Perfluorinated surfactants and the environmental implications of their use in fire-fighting foams. *Environmental science & technology* **2000,** *34*, 3864-3870.

3. Awad, E.; Zhang, X.; Bhavsar, S. P.; Petro, S.; Crozier, P. W.; Reiner, E. J.; Fletcher, R.; Tittlemier, S. A.; Braekevelt, E., Long-term environmental fate of perfluorinated compounds after accidental release at Toronto airport. *Environmental science & technology* **2011,** *45*, 8081-8089.

4. Hu, X. C.; Andrews, D. Q.; Lindstrom, A. B.; Bruton, T. A.; Schaider, L. A.; Grandjean, P.; Lohmann, R.; Carignan, C. C.; Blum, A.; Balan, S. A., Detection of poly-and perfluoroalkyl substances (PFASs) in US drinking water linked to industrial sites, military fire training areas, and wastewater treatment plants. *Environmental science & technology letters* **2016,** *3*, 344-350.

5. Mejia-Avendaño, S.; Munoz, G.; Vo Duy, S.; Desrosiers, M.; Benoît, P.; Sauvé, S.; Liu, J., Novel fluoroalkylated surfactants in soils following firefighting foam deployment during the Lac-Megantic railway accident. *Environmental science & technology* **2017,** *51*, 8313-8323.

6. Liu, M.; Munoz, G.; Vo Duy, S.; Sauvé, S.; Liu, J., Per-and polyfluoroalkyl substances in contaminated soil and groundwater at airports: a Canadian case study. *Environmental Science & Technology* **2021,** *56*, 885-895.

7. Cornelsen, M.; Weber, R.; Panglisch, S., Minimizing the environmental impact of PFAS by using specialized coagulants for the treatment of PFAS polluted waters and for the decontamination of firefighting equipment. *Emerging Contaminants* **2021,** *7*, 63-76.

8. Lang, J. R.; McDonough, J.; Guillette, T.; Storch, P.; Anderson, J.; Liles, D.; Prigge, R.; Miles, J. A.; Divine, C., Characterization of per-and polyfluoroalkyl substances on fire suppression system piping and optimization of removal methods. *Chemosphere* **2022,** *308*, 136254.

9. Krause, M. J.; Thoma, E.; Sahle-Damesessie, E.; Crone, B.; Whitehill, A.; Shields, E.; Gullett, B., Supercritical water oxidation as an innovative technology for PFAS destruction. *Journal of Environmental Engineering* **2022,** *148*, 05021006.

10. Hao, S.; Choi, Y.-J.; Wu, B.; Higgins, C. P.; Deeb, R.; Strathmann, T. J., Hydrothermal alkaline treatment for destruction of per-and polyfluoroalkyl substances in aqueous film-forming foam. *Environmental Science & Technology* **2021,** *55*, 3283-3295.

11. Pinkard, B. R., Aqueous film-forming foam treatment under alkaline hydrothermal conditions. *Journal of Environmental Engineering* **2022,** *148*, 05021007.

12. Place, B. J.; Field, J. A., Identification of novel fluorochemicals in aqueous film-forming foams used by the US military. *Environmental science & technology* **2012,** *46*, 7120-7127.

13. D'Agostino, L. A.; Mabury, S. A., Identification of novel fluorinated surfactants in aqueous film forming foams and commercial surfactant concentrates. *Environmental science & technology* **2014,** *48*, 121-129.

14. Barzen-Hanson, K. A.; Roberts, S. C.; Choyke, S.; Oetjen, K.; McAlees, A.; Riddell, N.; McCrindle, R.; Ferguson, P. L.; Higgins, C. P.; Field, J. A., Discovery of 40 classes of per-and

polyfluoroalkyl substances in historical aqueous film-forming foams (AFFFs) and AFFF-impacted groundwater. *Environmental science & technology* **2017,** *51*, 2047-2057.

15. Park, H.; Vecitis, C. D.; Cheng, J.; Choi, W.; Mader, B. T.; Hoffmann, M. R., Reductive defluorination of aqueous perfluorinated alkyl surfactants: effects of ionic headgroup and chain length. *The Journal of Physical Chemistry A* **2009,** *113*, 690-696.

16. Campbell, T. Y.; Vecitis, C. D.; Mader, B. T.; Hoffmann, M. R., Perfluorinated surfactant chain-length effects on sonochemical kinetics. *The Journal of Physical Chemistry A* **2009,** *113*, 9834-9842.

17. Bentel, M. J.; Yu, Y.; Xu, L.; Li, Z.; Wong, B. M.; Men, Y.; Liu, J., Defluorination of per-and polyfluoroalkyl substances (PFASs) with hydrated electrons: Structural dependence and implications to PFAS remediation and management. *Environmental science & technology* **2019,** *53*, 3718-3728.

18. Liu, Z.; Chen, Z.; Gao, J.; Yu, Y.; Men, Y.; Gu, C.; Liu, J., Accelerated Degradation of Perfluorosulfonates and Perfluorocarboxylates by UV/Sulfite + Iodide: Reaction Mechanisms and System Efficiencies. *Environmental Science & Technology* **2022,** *56*, 3699-3709.

19. Singh, R. K.; Multari, N.; Nau-Hix, C.; Woodard, S.; Nickelsen, M.; Mededovic Thagard, S.; Holsen, T. M., Removal of poly-and per-fluorinated compounds from ion exchange regenerant still bottom samples in a plasma reactor. *Environmental Science & Technology* **2020,** *54*, 13973-13980.

20. Zhuo, Q.; Deng, S.; Yang, B.; Huang, J.; Wang, B.; Zhang, T.; Yu, G., Degradation of perfluorinated compounds on a boron-doped diamond electrode. *Electrochimica Acta* **2012,** *77*, 17-22.

21. Schaefer, C. E.; Choyke, S.; Ferguson, P. L.; Andaya, C.; Burant, A.; Maizel, A.; Strathmann, T. J.; Higgins, C. P., Electrochemical Transformations of Perfluoroalkyl Acid (PFAA) Precursors and PFAAs in Groundwater Impacted with Aqueous Film Forming Foams. *Environmental Science & Technology* **2018,** *52*, 10689-10697.

22. Liang, S.; Mora, R.; Huang, Q.; Casson, R.; Wang, Y.; Woodard, S.; Anderson, H., Field demonstration of coupling ion-exchange resin with electrochemical oxidation for enhanced treatment of per-and polyfluoroalkyl substances (PFAS) in groundwater. *Chemical Engineering Journal Advances* **2022,** *9*, 100216.

23. Tenorio, R.; Liu, J.; Xiao, X.; Maizel, A.; Higgins, C. P.; Schaefer, C. E.; Strathmann, T. J., Destruction of per-and polyfluoroalkyl substances (PFASs) in aqueous film-forming foam (AFFF) with UV-sulfite photoreductive treatment. *Environmental science & technology* **2020,** *54*, 6957-6967.

24. Liu, Z.; Bentel, M. J.; Yu, Y.; Ren, C.; Gao, J.; Pulikkal, V. F.; Sun, M.; Men, Y.; Liu, J., Near-quantitative defluorination of perfluorinated and fluorotelomer carboxylates and sulfonates with integrated oxidation and reduction. *Environmental science & technology* **2021,** *55*, 7052-7062.

25. Gomez-Ruiz, B.; Gómez-Lavín, S.; Diban, N.; Boiteux, V.; Colin, A.; Dauchy, X.; Urtiaga, A., Efficient electrochemical degradation of poly-and perfluoroalkyl substances (PFASs) from the effluents of an industrial wastewater treatment plant. *Chemical Engineering Journal* **2017,** *322*, 196-204.

26. Schaefer, C. E.; Andaya, C.; Burant, A.; Condee, C. W.; Urtiaga, A.; Strathmann, T. J.; Higgins, C. P., Electrochemical treatment of perfluorooctanoic acid and perfluorooctane sulfonate: Insights into mechanisms and application to groundwater treatment. *Chemical Engineering Journal* **2017,** *317*, 424-432.

27. Lin, M.-H.; Bulman, D. M.; Remucal, C. K.; Chaplin, B. P., Chlorinated byproduct formation during the electrochemical advanced oxidation process at Magnéli phase Ti4O7 electrodes. *Environmental Science & Technology* **2020,** *54*, 12673-12683.

28. Shi, H.; Wang, Y.; Li, C.; Pierce, R.; Gao, S.; Huang, Q., Degradation of perfluorooctanesulfonate by reactive electrochemical membrane composed of magneli phase titanium suboxide. *Environmental science & technology* **2019,** *53*, 14528-14537.

29. Macpherson, J. V., A practical guide to using boron doped diamond in electrochemical research. *Physical Chemistry Chemical Physics* **2015,** *17*, 2935-2949.

30. Liu, Y.; Fan, X.; Quan, X.; Fan, Y.; Chen, S.; Zhao, X., Enhanced perfluorooctanoic acid degradation by electrochemical activation of sulfate solution on B/N codoped diamond. *Environmental science & technology* **2019,** *53*, 5195-5201.

31. Farhat, A.; Keller, J.; Tait, S.; Radjenovic, J., Removal of persistent organic contaminants by electrochemically activated sulfate. *Environmental Science & Technology* **2015,** *49*, 14326-14333.

32. Niu, J.; Li, Y.; Shang, E.; Xu, Z.; Liu, J., Electrochemical oxidation of perfluorinated compounds in water. *Chemosphere* **2016,** *146*, 526-538.

33. Radjenovic, J.; Duinslaeger, N.; Avval, S. S.; Chaplin, B. P., Facing the challenge of poly-and perfluoroalkyl substances in water: is electrochemical oxidation the answer? *Environmental Science & Technology* **2020,** *54*, 14815-14829.

34. Shende, T.; Andaluri, G.; Suri, R., Chain-length dependent ultrasonic degradation of perfluoroalkyl substances. *Chemical Engineering Journal Advances* **2023,** *15*, 100509.

35. Isowamwen, O.; Li, R.; Holsen, T.; Thagard, S. M., Plasma-assisted degradation of a short-chain perfluoroalkyl substance (PFAS): Perfluorobutane sulfonate (PFBS). *Journal of Hazardous Materials* **2023,** *456*, 131691.

36. Bentel, M. J.; Liu, Z.; Yu, Y.; Gao, J.; Men, Y.; Liu, J., Enhanced degradation of perfluorocarboxylic acids (PFCAs) by UV/sulfite treatment: Reaction mechanisms and system efficiencies at pH 12. *Environmental Science & Technology Letters* **2020,** *7*, 351-357.

37. Gao, J.; Liu, Z.; Chen, Z.; Rao, D.; Che, S.; Gu, C.; Men, Y.; Huang, J.; Liu, J., Photochemical degradation pathways and near-complete defluorination of chlorinated polyfluoroalkyl substances. *Nature Water* **2023,** *1*, 381-390.

38. Gao, J.; Liu, Z.; Bentel, M. J.; Yu, Y.; Men, Y.; Liu, J., Defluorination of Omega-Hydroperfluorocarboxylates (ω-HPFCAs): Distinct Reactivities from Perfluoro and Fluorotelomeric Carboxylates. *Environmental Science & Technology* **2021**.

39. Singh, R. K.; Multari, N.; Nau-Hix, C.; Anderson, R. H.; Richardson, S. D.; Holsen, T. M.; Mededovic Thagard, S., Rapid Removal of Poly- and Perfluorinated Compounds from Investigation-Derived Waste (IDW) in a Pilot-Scale Plasma Reactor. *Environmental Science & Technology* **2019,** *53*, 11375-11382.

40. Tenorio, R.; Liu, J.; Xiao, X.; Maizel, A.; Higgins, C. P.; Schaefer, C. E.; Strathmann, T. J., Destruction of Per- and Polyfluoroalkyl Substances (PFASs) in Aqueous Film-Forming Foam (AFFF) with UV-Sulfite Photoreductive Treatment. *Environmental Science & Technology* **2020,** *54*, 6957-6967.

41. Hao, S.; Choi, Y.-J.; Wu, B.; Higgins, C. P.; Deeb, R.; Strathmann, T. J., Hydrothermal Alkaline Treatment for Destruction of Per- and Polyfluoroalkyl Substances in Aqueous Film-Forming Foam. *Environmental Science & Technology* **2021,** *55*, 3283-3295.

42. Houtz, E. F.; Sedlak, D. L., Oxidative conversion as a means of detecting precursors to perfluoroalkyl acids in urban runoff. *Environmental science & technology* **2012,** *46*, 9342-9349.

43. García, R. A.; Chiaia-Hernández, A. C.; Lara-Martin, P. A.; Loos, M.; Hollender, J.; Oetjen, K.; Higgins, C. P.; Field, J. A., Suspect screening of hydrocarbon surfactants in AFFFs and AFFF-contaminated groundwater by high-resolution mass spectrometry. *Environmental science & technology* **2019,** *53*, 8068-8077.

44. Crittenden, J. C. T., R. R.; Hand, D. W.; Howe, K. J.; Tchobanoglous, G. , *MWH's Water Treatment: Principles and Design*, ; John Wiley & Sons, 2012.

45. Bentel, M. J.; Yu, Y.; Xu, L.; Kwon, H.; Li, Z.; Wong, B. M.; Men, Y.; Liu, J., Degradation of perfluoroalkyl ether carboxylic acids with hydrated electrons: Structure–reactivity relationships and environmental implications. *Environmental science & technology* **2020,** *54*, 2489-2499.

46. Yang, Y., Recent advances in the electrochemical oxidation water treatment: Spotlight on byproduct control. *Frontiers of Environmental Science & Engineering* **2020,** *14*, 85.

47. Gao, J.; Xie, S.; Liu, F.; Liu, J., Preparation and Synergy of Supported Ru0 and Pd0 for Rapid Chlorate Reduction at pH 7. *Environmental Science & Technology* **2023,** *57*, 3962-3970.

48. Ren, C.; Bi, E. Y.; Gao, J.; Liu, J., Molybdenum-Catalyzed Perchlorate Reduction: Robustness, Challenges, and Solutions. *ACS ES&T Engineering* **2022,** *2*, 181-188.

49. Yang, N.; Yang, S.; Ma, Q.; Beltran, C.; Guan, Y.; Morsey, M.; Brown, E.; Fernando, S.; Holsen, T. M.; Zhang, W.; Yang, Y., Solvent-Free Nonthermal Destruction of PFAS Chemicals and PFAS in Sediment by Piezoelectric Ball Milling. *Environmental Science & Technology Letters* **2023,** *10*, 198-203.

50. Li, X.; Ma, J.; Liu, G.; Fang, J.; Yue, S.; Guan, Y.; Chen, L.; Liu, X., Efficient reductive dechlorination of monochloroacetic acid by sulfite/UV process. *Environmental science & technology* **2012,** *46*, 7342-7349.

ACKNOWLEDGEMENTS

Financial support was provided by the Strategic Environmental Research and Development Program (ER22-3184 for Y.G., J.L., and Y.Y.) and the National Science Foundation (CBET-2120452 for S.Y. and Y.Y.).